NOTE: Use these buttons to print or save the form. DO NOT use the browser tool bar.

LA-UR-12-00676

Approved for public release;
distribution is unlimited.

Title:	MCNP6 Delayed-Particle Verification and Validation
Author(s):	Joe W. Durkee, Jr.
Intended for:	Code documentation.

Los Alamos
NATIONAL LABORATORY
EST.1943

Form 836 (7/06)

CLEAR FORM

LA-UR-12-00676

MCNP6 DELAYED-PARTICLE VERIFICATION AND VALIDATION
Rev 5: January 26, 2012

Joe W. Durkee, Jr.
Los Alamos National Laboratory
jdurkee@lanl.gov
505-665-0530
Fax: 505-665-2897
PO Box 1663, MS K575
Los Alamos, NM 87545

ABSTRACT

Updated verification and validation(v&v) testing of the MCNP6 delayed-particle feature, which includes treatment of delayed neutrons (DN) and delayed gammas (DG), was accomplished during the summer of 2011. These v&v tests were done in support of the MCNP/MCNPX code merger following two development issues. Issue 1 addressed the identification of MCNP6 and MCNPX coding differences. These differences included code changes that had been made to MCNPX but not MCNP6 prior to March, 2011, as well as faulty coding. Issue 2 pertained to the implementation of code in MCNP6 that had been tested solely in patch form with MCNPX (Durkee, June 2011). This patch was created in the wake of observations in March, 2011 that 1) the CINDER'90 (C90) CINDER interface routine (CID) did not treat more than one residual for DNDG creation by model (e.g., CEM) and 2) DN production was not invoked if DG production was not done for a particular fission or activation event. MCNP6 (load date June 9, 2011 version 6.2.08) and MCNPX 2.7.0 have been patched with coding to treat Issues 1 and 2. We refer here to the patched versions as MCNP6p and v270p. The v&v tests compare the MCNP6p (executed using dbcn(29)=1) and v270p results. The tests include 67

verification models and two experimental validation models. Twelve of these models treat HEU photofission. Included are calculations for DG production using either line or multigroup data and calculations without DG production. Half of the test set performed DN production via ACE library data, while the other half used the CID physics-model treatment. Twelve other models parallel the HEU photofission models, but treat thermal-neutron fission. The remaining six models treat DNDG production arising from 15-MeV neutron interaction with ^{17}O. The 37 (of 67) verification models test analog and implicit capture, behavior for a near-criticial model, and 800-MeV proton interaction with HEU, copper, and ^{18}O. The MCNP6 and v270p results compare favorably for all but one set of test problems wherein the inp01 test series revealed that MCNP6 does not correctly treat residual tallies. Validation tests were made using the Beddingfield and Cecil (1998) HEU and Pu experimental models. The MCNP6p and v270p validation results compare well with each other and with the measured high-resolution delayed-gamma data. The v&v test results discussed here complement results reported in the documents, "MCNP6 Delayed-Particle Verification and Validation" (LA-UR-11-01375, "MCNPX Delayed-Particle Verification and Validation" (LA-UR-11-03315) "MCNP6 Verification and Validation for MCNPX_65 and MCNPX_EXTENDED" (LA-UR-12-00179), and "The MCNP6 Delayed-Particle Feature" (LA-UR-12-00283).

KEYWORDS: MCNP6, MCNPX; delayed neutrons; delayed gammas; neutron fission; photofission.

1. Introduction

Los Alamos National Laboratory (LANL) develops and maintains the MCNP (Brown, 2003a; Brown, 2003b) and, prior to the merger, the MCNPX™(Pelowitz, 2008) Monte Carlo N-Particle eXtended general-purpose radiation transport codes. A merged version of MCNP and MCNPX, MCNP6, is expected to be released in 2012.

MCNP (MCNP6 and MCNPX) accommodates intricate three-dimensional geometrical models, continuous-energy transport of 36 different particle types plus heavy-ion transport, fuel burnup, and high-fidelity delayed-gamma emission. MCNP is written in Fortran 90, has been parallelized, and works on platforms including single-processor personal computers (PCs), Sun workstations, Linux clusters, and supercomputers. MCNP has approximately 10000 users[†] throughout the world working on endeavors that include radiation therapy, reactor design, and homeland security.

MCNP provides users with self-contained calculations involving delayed-neutron (DN), delayed-gamma (DG), or delayed-neutron and delayed-gamma (DNDG) emission. The feature has been developed to make it as simple as possible to use, but provide the user with versatility and flexibility. The DNDG feature is thus complicated because of the number of execution options, the DG data types, and availability of DG line data. Depending on the execution options, the DNDG feature can also be time-consuming to execute. A good deal of effort has been expended to improve execution performance, and additional work can be done to further reduce execution time. Some of the theoretical,

[†] Tim Goorley email of October 4, 2011.

computational, and data development effort supporting the MCNPX DG feature is detailed in the literature (Durkee et al., 2009a, 2009b). We recap and examine the DNDG feature and the issues associated with DNDG v&v in the following two Sections.

2. DNDG feature

With the objective of maximizing performance, our development of the DNDG feature has been influenced by the following interesting characteristic: for any given problem, a semi-finite number of fission products (FPs) or residuals exist. Recall the classic double-hump fission yield curve (Lamarsh, 1972). For MCNP simulations involving fission, there are about 300–400 FPs that are recurrently sampled over 99% of the time. The remaining FPs are rarely sampled. This means that cumulative distribution functions (CDFs) for these frequently sampled FPs can be calculated once, stored, and reused for DNDG emission sampling. This calculate, store, and reuse strategy is efficient because the use of CINDER'90 and the execution of the nested DO loops are time consuming computer-intensive operations.

Because of the interest in interrogation applications, this calculate, store, and reuse algorithm has been implemented for thermal-neutron fission of ^{235}U and ^{239}Pu. MCNPX calculations were done during feature development to sample the most frequently sampled FPs. These data are stored at the top of the delayed-particle CINDER'90 interface routine "CID." During execution, sampling of the most frequently FPs causes their CDFs to be built, saved, and reused during subsequent histories where such FPs are

sampled. In this manner, execution time is reduced by over 90% versus execution without the CDF calculate, store, and reuse strategy. This algorithm is implemented in MCNP6.

This calculate, store, and reuse algorithm has been implemented only for the FPs created by thermal-neutron fission of ^{235}U and ^{239}Pu. An upgrade to dynamically determine the most frequently sampled FPs on a model-dependent basis has yet been done.

Simulation models involving activation events [e.g., (n,p), (p,α), etc.) often have a wide assortment of materials other than ^{235}U and ^{239}Pu. MCNPX versions prior to 2.7.d (v27d) lacked a CDF build, save, and reuse strategy for activation reactions. Consequently, for each activation event the CDF was calculated, DNDG emission done, and the CDF was not stored for reuse. The CDFs for all activation products had to be repeatedly calculated, which appreciably slowed execution.

Beginning with MCNPX v27d, an algorithm was implemented to enable MCNPX to dynamically determine the most frequently sampled activation products (APs) (Durkee et al., 2010). The list of APs is updated during execution, and the CDFs for the most frequently sampled activation products are stored. CDFs for less frequently sampled APs are calculated on an event-by-event basis. This algorithm, which is implemented in MCNP6, results in reductions of execution time ranging from 75% to well over 90%.

This AP algorithm treats events producing a single residual. In some simulations, physics-model invocation can cause the production of two or more residuals per event. An upgrade to treat events with more than one AP residual has not yet been done.

Counterbalancing the CDF calculate, store, and reuse strategies are storage limitations. For the low-resolution multigroup (MG) DG option, modern computers can store the CDFs for all 3400 nuclides treated by CINDER'90. Unfortunately, capacity is inadequate to permit CDF storage for all FPs and APs when high-resolution line DG simulations are executed. Consequently, as discussed in the preceding paragraphs, CDF storage schemes have been developed to save the most frequently sampled FPs and residuals. These schemes add a good deal of complexity to the coding.

Calculations treating DG emission are further complicated (Durkee et al., 2009a) because of 1) two types of emission data: 25-group (MG) and line, 2) two energy CDF integration schemes: MG and "exact" (line-by-line),[†] and 3) CDF storage strategies for FPs and APs. The user can request either low- or high-resolution simulations.

For MG (low-resolution) execution, a single DG emission dataset (25-group from cinder.dat) is used, a single (MG) integration strategy is used, and the energy CDFs are calculated and stored for all fission or activation events.

[†] This refers to the CDFs created and sampled for the emission energy of each DG. CDFs are also created for sampling of the emission time of each DG.

For line (high-resolution) execution, the line dataset (cindergl.dat) contains data for only 979 nuclides. For the remaining nuclides, the MG data (cinder.dat) are used. Consequently, algorithms and infrastructure have been developed to treat hybrid CDFs consisting of line and MG components. For each fission or activation event, the CDF for each FP or residual can consist of all DG line data, MG data, or a mixture of DG and MG data. The CDF integration scheme and storage strategy must accommodate these various data issues (Durkee et al., 2009a).

The DNDG feature operates in concert with additional features including 1) neutron transport with analog or implicit capture, 2) analog or biased DN production, 3) the use of residual tallies, 4) neutron fission or photofission, and 5) residual creation by sampling of library data or physics models.

Although the DNDG model-based algorithm is Monte Carlo, CDF calculation uses a numerical (trapezoidal rule) scheme (Durkee et al., 2009a) to approximate the time integral of the atom densities. Recent advances (Durkee et al., 2010) now permit analytic integration for events with residuals having no radioactive decay products. Numerical integration is used for events with residuals that have radioactive decay products.

The MCNP6 DNDG feature thus contains an assortment of data and algorithms, which complicates the process of verifying and validating the DNDG feature. Many of these factors are summarized in bullet form below.

DN Production

- DN production can be done using either ACE data (acedel.F) or the C90 model calculation (the CID module and cinder.dat "pn" DN emission data for each DN emitter). DN production for models with photonuclear reactions can be done only using the C90 model option (there are no calls to acedel.F90 from collpn.F90 to permit DN production using ACE data).
- DN production can be analog or biased.

DG Production

- 25-group (dgb=–101[†]): single MG (25-group) dataset, MG integration CDF, CDF stored for all 3400 nuclides.
- Line (dgb=–102): line data augmented by MG data, hybrid MG and line CDF, hard-coded CDF storage for most frequently sampled FP pairs, dynamic CDF storage for most frequently sampled single APs or residuals, complicated storage for most frequently sampled FPs and APs plus treatment for infrequently sampled FPs and APs.
- DG production is complicated because of the assortment of emission data, cumulative distribution sampling (CDF) integration schemes, and CDF storage strategies. The user can request either low- or high-fidelity simulations. The simulations involve 25-group (MG) data or line emission data, cumulative

[†] The test problems used the PHYS:n dnb and the PHYS:p card dgb input parameters to control DN and DG production in the test models. Equivalently, these DN and DG production can be controlled using the ACT card "DN" and "DG" keywords and options. For example, dgb=–101 and dgb=–102 correspond to ACT DG=MG and ACT DG=LINES, respectively. Historically, the physics-card switches were created prior to the development of the ACT card.

distribution sampling (CDF) integration schemes for energy and time emission, and CDF storage strategies.

- Neutron fission or photofission data.

DNDG Production

- Execution for DN, DG, or DN and DG.
- Execution for FP, AP, or FP and AP.
- Execution for neutron transport using analog or implicit capture.
- Execution option to include residual tallies.

3. MCNP6 delayed-particle code modifications

Two key code-development issues issues had to be resolved during MCNP6 6.2.08 v&v. These issues involved 1) coding differences between MCNP6 and MCNPX and 2) coding upgrades to address DNDG modeling deficiencies.

3.1. Issue 1: Code difference identification.

This issue was addressed by first modifying copies of the MCNP6 and v270 delayed-particle modules cinder_mod.F90 and GLOBAL6_mc.F using a text editor to remove superfluous differences (e.g., indentations, trailing "&" for MCNP6 continuation statements, etc.). The UNIX "diff" command was then executed using the modified files to locate coding differences. The process identified approximately ten code bugs in MCNP6 that were corrected.

3.2. Issue 2: Implementation of March, 2011 DNDG upgrades.

Modifications that had been developed to correct MCNPX DNDG code deficiencies (Durkee, June 2011) were implemented in MCNP6 and v270p. These modifications include:

- DN and/or DG production for multiple residuals produced via C90 model calculations are now treated with the CID "nflag=2 nzero fix". This fix calculates CDFs for all nzero residuals for events involving 1) activation or 2) model-based residual creation (e.g., fission calculated using CEM).
- DN emission is now treated for events when DG emission does not occur. The pre-fix MCNP6 and MCNPX v270 treated DN emission for calculations for which DG was not requested (dgb=0[†]), but skipped DN emission for histories when FP or residuals lacked DG data. For some models, the code upgrade will result in little or no additional DN production. Higher DN production for MCNP6p and v270p versus pre-fix version could occur if prominent DN producers were not being treated.
- For FP or activation events involving multiple residuals, when at least one residual is stable the CDF is now calculated for the unstable residual(s). Pre-fix versions skipped the CDF creation and DG emission for an entire fission or activation event if any residual was stable.
- For FP or activation events involving multiple residuals, when all residuals are unstable but one or more lacks DG data the CDF is now created for any other

[†] This is equivalent to ACT DG=NONE.

unstable residual that has DG data. Pre-fix versions skipped the CDF creation and DG emission for an entire fission or activation event if all residuals were unstable but any residual lacked DG data.

4. MCNP6 delayed-particle verification and validation

The v&v process required to comprehensively check all of the capabilities and combinations of capabilities listed in the preceding two Sections is formidable. Compounding the complexity is the reality that much of the capability was first developed in several stages during the 2005–2011 timeframe in MCNPX and then merged into MCNP6 at various times during the course of the merger effort. Moreover, formatting changes were made to the ported code during merging, which renders a simple side-by-side comparison of MCNP6 and MCNPX coding tedious and difficult. The inclusion of coding to treat Issues 1 and 2 further complicates the v&v process.

The MCNP6 v&v work done here proceeded as follows. MCNP6p and v270p were used to execute and compare results for v&v simulations using 67 verification models and two experimental validation models.

The verification calculations were executed using an Intel serial build (make build CONFIG="intel plot acode msvc" with debugging) on the PC. The validation calculations were executed using a Portland group MPI build on the Pete cluster.

Perl scripts were written to automate MCNP6p and v270p execution and perform UNIX "diff" operations on output ("outp") and tally ("mctal") files. Visual inspection of "Problem Summary" table data also was done. This inspection process is tedious, and can result in overlooked problems. During the past several years, numerous plots of spectra calculated using MCNPX have been made. Such plots have been beneficial in identifying problems. Within the limited time available for this study, plots of results were produced only for the validation models based on the Beddingfield and Cecil experiments (1998).

The next two sections describe the verification and validation models. Section 5 delineates the results. The most outstanding problems are highlighted using a red font. Important fixes to previous v&v reports are highlighted using a green font. Conclusions and a list of citations conclude this report. This work was done during July and August 2011.

4.1. Verification models.

Seven sets of models are used for verification calculations. We have no measured data against which to compare the calculated results for these models.

The first set has three models for activation and fission and involve irradiation of ^{18}O, natural copper, and HEU by 800-MeV protons. These are referred to as the "LSW" models.

Test set two consists of five activation models containing ^{27}Al, ^{58}Ni, ^{60}Ni, ^{16}O, and ^{94}Zr. Each target is bombarded by 15-MeV neutrons. These are the simple multiparticle "SMR" models.

Test set three has one test model, referred to as the "DBP" model ("dbp3del"), used to test the DNDG feature for subcritical systems whose keff is "near" unity (~0.9). This model is executed in source (SDEF) mode. This model came to light when execution using the 2009 MCNPX 2.7.a.3 version caused the calculation to "hang" without completion. The issue at that time was caused by neutron conservation issues for models with TOTNU and DN produced using the C90 model. In effect, accounting issues resulted in excess neutrons, which in turn led to artificially elevated reactivity. Modifications to MCNPX subroutines acedel.F, acecol.F, colidn.F, dng_model.F, and CID were made during that timeframe to fix the problem. In the wake of those modifications, the test models executed without hanging. Additional modifications were then made to correct accounting issues that were evident in the Problem Summary Table. Those fixes permitted exact accounting for all neutrons (source and loss). The corrected accounting then permitted the calculation of reasonable values of the average total delayed neutron fraction, $\overline{\beta}$.[†]

Test set four has twenty-eight models that are used to test analog and implicit capture with and without delayed-particle emission and with the F8 residual tally. These are the "ACIC" models.

[†] This differs from the effective delayed neutron fraction, a quantity that is developed using adjoint-weighting in a point-kinetics formulation (Bell and Glasstone, 1970; Hetrick, 1971; Massimo, 1976; Henry, 1975).

Test sets five through seven contain 30 models. These sets are designed to test 1) C90 model (nflag=2) DNDG production, including multiple residuals (nzero > 1), and 2) the fixes for DN production in the absence of DG production. Test set 5 contains twelve models that treat HEU photofission by 12-MeV photons. Two main subsets treat DN production by 1) ACE data (dnb=–1) or 2) C90 model (dnb=–101).† These subsets are each divided into DG production by data (CID nflag=1) or model (CEM nflag=2), and DG production is done by line (dgb=–102), MG (dgb=–101), or off (dgb=0). Test 6 has twelve models that treat HEU neutron fission by 0.025-eV neutron with DN production. The two main subsets for DN production are by 1) ACE data (dnb=–1) or 2) C90 model (dnb=–101), For each subset, DG production by data (CID nflag=1) or model (CEM nflag=2), and DG production is done by line (dgb=–102), MG (dgb=–101), or off (dgb=0). Test set 7 contains six models that test DNDG production for ^{17}O irradiated by 15-MeV neutrons. DN production by 1) ACE data (dnb=–1) or 2) C90 model (dnb=–101), and DG production for each is done by line (dgb=–102), MG (dgb=–101), or off (dgb=0).

All models in sets five through seven are executed with the request that DNDG production be done for activation products in addition to (the default) fission products. CDFs for the top 50 most frequently sampled individual (nzero=1) activation or residual products (nflag=2) are to be saved for reuse. These specifications are made using the act card:

act nonfiss=all nap=50

† The PHYS:N dnb= –1 and dnb= –100 specifications are equivalent to ACT DN=LIBRARY and ACT DN=MODEL, respectively, without the ACT card DNBIAS keyword. This causes analog DN emission using ACE library data and CINDER'90 models, respectively.

4.2. Validation models.

In previous work, we developed the theory (Durkee et al., 2009a) and reported simulation results (Durkee et al., 2009b; Durkee et al., 2009c) pertaining to the delayed-gamma experiments reported by Beddingfield and Cecil (1998). The experiments involved the irradiation of stationary HEU and Pu targets by a moderated ^{252}Cf neutron source. Because many of the details of their experiments were not provided, we approximated the experimental setup by using a 0.025-eV neutron pulse directed inwardly from a spherical surface source. In addition, because details of their HPGe detector were unavailable, we also developed a simulated detector using representative parameters. Despite our modeling approximations, our simulation results proved to be in quite good agreement with their measured spectra for HEU and Pu. The HEU and Pu models are revisited here using MCNP6p and v270p.

5. Verification and validation results

Computational results obtained using the verification and validation models are presented in the following subsections. These tests were done using MCNP6 and v270p built with the Issue 1 and 2 coding fixes. Here we do not address differences (usually increases) in DNDG production for MCNP6 and v270 builds made 1) with and 2) without the Issue 2 capability. The v270p results in this report are identical to the results discussed in the MCNPX v&v document (Durkee, June 2011). Thus, the interested reader can refer to that document to examine differences in DNDG production attributable to the

Issue 2 fixes. In this document, we focus our attention on the results obtained using MCNP6P and v270p inclusive of Issue 1 and 2 coding.

For tracking purposes, the following information is of note. Perl scripts were written to execute the calculations and perform UNIX "diff" operations on the outp and mctal files generated by MCNP6p and v270p. The PC executable and test files are located on the directory

095536@pn1176518 /cygdrive/c/MCNP60602/MCNP6/runjbs

under six subdirectories named ACIC, BEDD_NEUTFISS, BEDD_PHOTOFISS, DBP, LSW, and SMRS. The MPI executables and test files for the Beddingfield validation calculations are on the PETE cluster in directories:

/home/jdurkee/old_pete/MCNP60602/MCNP6/runjbs

/home/jdurkee/old_pete/MCNPXv270/v270m6mP/src/mcnpx/runjbs/RDISK/F8

5.1. Test Set 1: LSW models.

The first set of models test activation and fission. These models were used during the development of the DG speedup upgrades for models with activation reactions during 2010 (Durkee et al., 2010).

These models contain the "phys" cards

```
phys:n 800 j j -101 j 1      $ delayed analog sampling models
```

phys:p j j j -1 j -102 $ analog photonuclear & multigoup delayed

and the "act" card "act nonfiss=all nap=40" for o18lsw, culsw, and heulsw.

Results for the LSW activation models are listed in Table 1.1. The outp file Problem Summary data are reasonable for o18lsw, culsw, and heulsw. Differences are likely attributable to random number sequencing. **The o18lsw DN creation by fission is identical (30 for this model) for both MCNP6p and v270p. In the earlier v&v work (Durkee, February 2011, Table 1), the MCNP6 result was nil. During the course of the present work it was noted that MCNP6p execution must be done using TOTNU, which rectified the discrepancy between the MCNP6p and v270p results without TOTNU (0 DN for MCNP6p, 30 DN for v270p). The requirement that TOTNU be used in (inp files for) models that treat activation without fission is not intuitive and should be revisited in future code (see Conclusions for the recent beta 2 release). During testing of heulsw a code bug was identified and corrected.**[†]

Table 1.1 Results for LSW test models.

Test Model	Results for MCNP6p and v270p			
	Problem Summary table		mctal file	Other
	MCNP6p	v270p		
o18lsw	DN 30 DG 65	DN 30 DG 75	Differences	
culsw	DN 0 DG 664	DN 0 DG 673	Differences	No DN, as desired.
heulsw	DN 0 DG 485	DN 0 DG 466	Differences	Inefficient DN producer

[†] This error was found using the Intel compiler with a debug build to flag array-bounds errors. Coding in subroutine loadlines_this_fpc was changed from espkgl_fpc(i,il,1) to espkgl_fpc(idespkgl(i),il,1).

The discrepancy in the DG results obtained using MCNP6p and v27p for o18lsw was examined using a series of tests using 10^4, 10^5, and 10^6 source histories. The results, shown in Table 1.2, indicate converging behavior, as desired.

Table 1.2. Results LSW o18lsw test model as a function of NPS.

Test Model	Results for MCNP6p and v270p					
	NPS	Problem Summary table: tracks				Percent difference
		MCNP6p		v270p		
o18lsw	10^3	DN	30	DN	30	0
		DG	65	DG	75	-13
	10^4	DN	328	DN	329	-0.3
		DG	774	DG	817	-5.2
	10^5	DN	3249	DN	3261	-0.3
		DG	7137	DG	7426	-3.9
	10^6	DN	32235	DN	32280	-0.1
		DG	73187	DG	76103	-3.8

Execution time ranges from less than 1 minute for 10^3 histories to several hours for 10^6 histories.

5.2. Test Set 2: SMR activation models.

The second set of test problems test simple multiparticle activation. These models contain the "phys" cards

```
phys:n 3j -1        $ Analog sampling, libraries only.
phys:p 5j -102      $ MG + Line.
```

and the "act" card "act nonfiss=p nap=4" for ni58del, "act nonfiss=all nap=1" for ni60del, "act nonfiss=p nap=10" for o16del, "act nonfiss=p" for al27del, and "act nonfiss=p nap=10" for zr94del.

Results for this set of test problems are listed in Table 2. The outp Problem Summary data are identical for all test problems. The mctal file data have small statistical differences for a few tally values. Results are consistent with expectations.

Table 2. Results for SMR test models

Test Model	Results for MCNP6p and v270p		
	Problem Summary table	mctal file	Other
ni58del	Same	A few values differ slightly, maybe fom	
ni60del	Same	A few values differ slightly, maybe fom	
o16del	Same	A few values differ slightly, maybe fom	
al27del	Same	A few values differ slightly, maybe fom	
zr94del	Same	A few values differ slightly, maybe fom	

5.3. Test Set 3: DBP model.

The DBP model was used in early 2009 to debug and upgrade the treatment of DNs. This model contains enough fissile material to reveal that MCNPX had deficiencies that caused calculations to exhibit artificial and erroneous supercriticality. Debug tests made at that time showed histories that had huge numbers of progeny neutrons created. Calculations would "hang" because such histories would never conclude. The root cause of the behavior was the improper handling of neutron balance. For models with TOTNU, the total number of neutrons created by a fission event was calculated in acecol.F. Next, the number of delayed neutrons was calculated in dng_model.F. The collision multiplicity (cmult) was then calculated as the sum of the total and delayed neutrons produced by a fission event. Also, in an ensuing loop the total number of neutrons from a fission event was used in the call to acecas.F. Coding was modified to 1) calculate the

number of prompt neutrons = total – delayed for an event for the acecas.F loop, and 2) set cmult to the total number of neutrons for a fission event (the existing coding added the delayed to the total). In addition, colidn.F required modification to treat the case in which a single neutron that is a delayed neutron is produced by an event. This required modifications to properly update accounting for the Problem Summary table. Once these fixes were made, this faulty behavior vanished and dbp3del executed. These modifications have been used in MCNP6p and v270p.

The DBP model includes the phys cards

```
phys:p    j j j -1 j -102
phys:n  100 j j -101 j 1  0
```

and no "act" cards (so no DN and DG from activation, only from fission). These models contain photon sources ("si" and "sp" distributions).

Table 3.1 contains results for the DBP model executed using 10^6 source histories to achieve modest statistics. Execution with MCNP6p and v270p was successful insofar as execution concluded and did not "hang". Each calculation required approximately 1 hour of CPU time on the PC.

The calculated $\overline{\beta}$ values were an important factor in determining whether the upgrades function correctly. $\overline{\beta}$ for dbp3del using MCNP6p is calculated to be $\overline{\beta}$ =4.7817e-7/(4.7817d-7+6.5095e-5)=7.292e-3 [calculated using the summary table "prompt fission" and "delayed fission" weights as delayed wt/(prompt + delayed)], and nu=2.60 (from print table 117). For v270p, $\overline{\beta}$ =6.1833e-7/(6.1833d-7+7.8966e-

5)=7.769e-3. The Lamarsh values for fast neutron-induced fission of ^{235}U and ^{238}U are 0.0064 and 0.0148, respectively.† Thus, it appears that $\bar{\beta}$ calculated using MCNP6p and MCNPX v270p are reasonable, though not identical.

Table 3.1. Results for DBP test model dbp3del using 10^6 source histories.

Test Model	Results for MCNP6p and v270p				
	Problem Summary table		mctal file	$\bar{\beta}$	
dbp3del	MCNP6p	v270p		MCNP6p	v27p
	DN 232 DG 83138	DN 300 DG 99847	Many differences	7.292e-3	7.769e-3

DN and DG production for MCNP6p listed in Table 3.1 are approximately 17% and 23% lower than v270p, respectively. This model uses a photon source and a W convertor. Thus, it is possible that the differences are attributable to differences in the MCNP6p and v270p physics package results. To assess convergence behavior, dbp3del was executed for large numbers of histories. Execution was done with Portland Group MPI builds on the Pete cluster using 48 processors. The results Problem Summary table data, listed in Table 3.2, indicate converging behavior, as desired. For the 10^9 source-history calculations, $\bar{\beta}$ =5.1836e-7/(5.1836d-7+6.7653e-5)=7.604e-3 and 5.5107e-7/(5.5107d-7+6.8190e-5)=8.017e-3 for MCNP6p and v270p, respectively, which are reasonable.

† Values for v27a3, the first MCNPX version for which the modifications to correct the delayed-neutron treatment were made, were $\bar{\beta}$ =7.641e-3=5.3514e-7/(6.96e-5+5.3514e-7)] and nu=2.59.

Table 3.2. Results DBP test model dbp3del as a function of NPS for a Portland Group MPI build on the Pete cluster executed using 48 processors.

Test Model	Results for MCNP6p and v270p					
	NPS	Problem Summary table: tracks				Percent difference
		MCNP6p		v270p		
dbp3del	10^6	PN	31915	PN	31099	+2.6
		DN	256	DN	250	+2.4
		DG	83572	DG	81942	+2.0
	10^7	PN	311697	PN	344293	-9.5
		DN	2371	DN	2778	-15
		DG	819117	DG	900955	-9.1
	10^8	PN	3250101	PN	3325879	-2.3
		DN	24941	DN	27090	-7.9
		DG	8524074	DG	8728628	-2.3
	10^9	PN	32823284	PN	33084060	-0.8
		DN	251494	DN	267364	-5.9
		DG	86066898	DG	86804246	-0.9

Execution time ranges from 20 minutes for 10^6 histories to several hours for 10^9 histories.

5.4. Test Set 4: ACIC models.

Test set 4 contains many decks to test analog and implicit capture with and without the ft8 residual tally. Test set 4 contains 6 subsets.

5.4.1. ACIC subset 4a.

Subset 4a decks contain 50/50 ^{235}U and ^{238}U and a 7-MeV neutron source. Decks inp01ac and inp01ic contain delayed + ft8, inp01acd and inp01icd delayed only, and inp01ac8 and inp01ic8 ft8 residual-tally only (phys:n 3j 0, and phys:p card commented). There is no "act" card in any of the input files. The following phys cards are used:

```
phys:n 3j  101  $ Delayed neutrons using C90
```

phys:p 5j -101 $ Delayed gammas using multigp data

Table 4a.1 contains results for the analog and implicit capture tests calculated using 1000 source histories. There are many differences in the outp file Problem Summary table (PST) results for prompt neutrons from fission (PN), delayed neutrons from fission (DN), and delayed gammas (DG). Moreover, the residual tallies for each of the six models are zero for MCNP6p—which is incorrect—and nonzero for v270p. Models inp01ac, inp01ic and inp01ac8, inp01ic8 (rows 1,2 and 5,6) each calculate residuals (inp01ac and inp01ic also calculate DN and DG).Thus, the differences in the PST values for these models calculated using MCNP6p and v270 might be attributable to the residual error in MCNP6.

Inspection using debug triggers in talres.F90 shows that the values for jptal and lft (basic tally info and pointers to the FT-card data, respectively) are incorrect for MCNP6, differing from MCNPX. Mike James says this issue has not yet been fixed for MCNP6.

Models inp01acd and inp01icd (rosw 3,4) do not include a residual tally. So the differences in the PST results for these models cannot be attributed to a faulty residual tally. Table 4a.2 contains results calculated using these models for 10^3, 10^4, 10^5, and 10^6 source histories. The PST results for MCNP6p and v270p tend to converge as the number of histories increases. This behavior suggests that for this pair of models MCNP6p is functioning correctly.

Table 4a.1. Results for analog and implicit capture inp01 series test models for NPS=1000.

Test Model	Results for MCNP6p and v270p			
	Problem Summary table: tracks		mctal file	Other
	MCNP6p	v270p		
inp01ac	PN 915 DN 193 DG 3101 **All residuals ZERO**	PN 879 DN 206 DG 3100 **Nonzero residuals**	Many differences	
inp01ic	PN 639 DN 136 DG 2185 **All residuals ZERO**	PN 1057 DN 226 DG 3601 **Nonzero residuals**	Many differences	
inp01acd	PN 601 DN 127 DG 1986 Many other differences.	PN 729 DN 164 DG 2497	Many differences	No residuals, as desired.
inp01icd	PN 2696 DN 591 DG 9923 Many other differences.	PN 2157 DN 489 DG 7541	Many differences	No residuals, as desired.
inp01ac8	PN 615 DN 0 DG 0 **All residuals ZERO**	PN 1141 DN 0 DG 0 **Nonzero residuals**		No DNDGs as desired
inp01ic8	PN 852 DN 0 DG 0 **All residuals ZERO**	PN 726 DN 0 DG 0 **Nonzero residuals**		No DNDGs as desired

Table 4a.2. Results for analog and implicit capture inp01 series test models as a function of NPS.

Test Model	Results for MCNP6p and v270p			
	NPS	Problem Summary table: tracks		Percent difference
		MCNP6p	v270p	
inp01acd	10^3	PN 601	PN 729	–17
		DN 127	DN 164	–22
		DG 1986	DG 2497	–20
	10^4	PN 9536	PN 11157	–14
		DN 2083	DN 2361	–12
		DG 32701	DG 38748	–16
	10^5	PN 101097	PN 106200	–4.8
		DN 21617	DN 22594	–4.3
		DG 346358	DG 363529	–4.7
	10^6	PN 1038218	PN 1061073	–2.1
		DN 220340	DN 224712	–1.9
		DG 3561338	DG 3637730	–2.1
inp01icd	10^3	PN 2696	PN 2157	+25
		DN 591	DN 489	+21
		DG 9923	DG 7541	+31
	10^4	PN 11355	PN 12936	–12
		DN 2406	DN 2803	–14
		DG 39746	DG 44548	–11
	10^5	PN 118929	PN 120585	–1.4
		DN 25444	DN 25749	–1.1
		DG 409013	DG 415705	–1.6
	10^6	PN 1116797	PN 1127159	–0.9
		DN 238214	DN 240164	–0.8
		DG 3855328	DG 3895308	–1.0

CPU time ranges from less than 1 minute for 10^3 histories to several hours for 10^6 histories.

5.4.2. ACIC subset 4b.

Subset 4b inp files contain HEU. The phys cards are

```
phys:n 3j -101
phys:p 5j -101
```

and the source is a Watt fission spectrum

```
sdef  par=n erg=d1 sur=2 nrm=-1
```

sp1 -3

There is no “act” card.

The results in Table 4b show that the MCNP6 and v270p results for each test model agree in general. Some differences between analog and implicit capture results are noted for each model; however, these differences may be due to statistics.

Table 4b. Results for analog and implicit capture inp04 series test models.

Test Model	Results for MCNP6p and v270p			
	Problem Summary table		mctal file	Other
	MCNP6p	v270p		
inp04ac	PN 706 DN 4 DG 2349 Others close 6 & X.	PN 711 DN 3 DG 2351	Many small differences	Residuals close for 6 and X.
inp04ic	PN 730 DN 5 DG 2427 Other 6 & X close.	PN 735 DN 4 DG 2429	Many small differences	Residuals close for 6 and X.
inp04acd	PN 713 DN 4 DG 2387 Other 6 & X identical.	PN 713 DN 4 DG 2387	Few small differences	No residuals, as desired.
inp04icd	PN 650 DN 5 DG 2188 Other 6 & X identical.	PN 650 DN 5 DG 2188	Few small differences	No residuals, as desired.
inp04ac8	PN 425 DN 0 DG 0 Other 6 & X close.	PN 428 DN 0 DG 0	Few differences, perhaps fom	Residuals close for 6 and X.
inp04ic8	PN 443 DN 0 DG 0 Other 6 & X close.	PN 446 DN 0 DG 0	Few differences, perhaps fom	Residuals close for 6 and X.

5.4.3. ACIC subset 4c.

Test set 4c contains a 3.975-cm sphere of ^{16}O. The phys and act cards are

```
phys:n 3j -1        $ Analog sampling, libraries only.
phys:p 5j -102      $ MG + Line.
act nonfiss=p
```

A volumetric source of 15-MeV neutrons is distributed throughout the ^{16}O sphere.

The MCNP6p and v270p outp file problem summary table results are the same for the respective analog- and implicit-capture models. As expected, both MCNP6p and v270p give elevated DG production for implicit versus analog capture. This DG-production behavior occurs because, for implicit capture, the neutrons continue to be tracked following capture reactions, and DGs are produced for each capture reaction. For analog capture, DGs are produced only for the single (initial) capture events. The implicit-capture DGs have lower weight associated with the weight of the neutrons inducing the capture reactions.

Table 4c. Results for analog and implicit capture inp20 series test models.

Test Model	Results for MCNP6p and v270p		
	Problem Summary table	mctal file	Other
inp20ac	Same	Few differences, perhaps fom	
inp20ic	Same. 381 DG IC vs 40 for AC. IC DG weights lower vs AC.	Few differences, perhaps fom	
inp20acd	Same	Few differences, perhaps fom	
inp20icd	Same. 381 DG IC vs 40 for AC. IC DG weights lower vs AC.	Few differences, perhaps fom	
inp20ac8	Same	Few differences, perhaps fom	No DNDGs as desired
inp20ic8	Same	Few differences, perhaps fom	No DNDGs as desired

5.4.4. ACIC subset 4d.

Test set 4d contains ^{3}He and a 10-MeV neutron source. The phys and act cards are

```
phys:n 3j -1        $ Analog sampling, libraries only.
phys:p 5j -102      $ MG + Line.
act nonfiss=p
```

This model is designed to test the residual tally for the $^{3}He(n,^{2}H)^{2}H$ and $^{3}He(n,^{1}H)^{3}H$ reactions. There is no DN or DG production for this model. As indicated in Table 4d, the results look good. Some differences between MCNP6p and v270p are observed in the outp and mctal files for the "if the largest history score sampled so far were to occur on the next history, the tfc bin quantities would change as follows" figure-of-merit values. The residual tallies are identical for MCNP6p and v270p, as desired.

Table 4d. Results for analog and implicit capture inp21 series test models.

Test Model	Results for MCNP6p v270p		
	Problem Summary table	mctal file	Other
inp21ac	Same	Only FOM for TFC	Identical ^{2}H and ^{3}H residual tallies
inp21ic	Same	Only FOM for TFC	Identical ^{2}H and ^{3}H residual tallies

5.4.5. ACIC subset 4e.

Test set 4e contains ^{10}B with a 10-MeV neutron source. The phys and act cards are

```
phys:n 3j -1 2j 2   $ Analog sampling, libs only, Li+NCIA.
phys:p 5j -102      $ MG + Line.
act nonfiss=p
```

This model tests residual production in the absence of DN and DG production. As delineated in Table 4e, these computational results for the each model obtained using MCNP6p and v270p are identical. Some differences between MCNP6p and v270p are observed in the outp and mctal files for the "if the largest history score sampled so far were to occur on the next history, the tfc bin quantities would change as follows" figure-of-merit values. The residual tallies are identical for MCNP6p and v270p, as desired.

Table 4e. Results for analog and implicit capture inp22 series test models.

Test Model	Results for MCNP6p and v270p		
	Problem Summary table	mctal file	Other
inp22ac	Same	Only FOM for TFC	No DN, DG. Residuals tallied for ^{4}He, ^{7}Li, ^{9}Be, ^{10}Be are identical for d &dp.
inp22ic	Same	Only FOM for TFC	No DN, DG. Residuals tallied for ^{4}He, ^{7}Li, ^{9}Be, ^{10}Be are identical for d & dp.
inp22acd	Same	Only FOM for TFC	No DN, DG. No residuals as desired
inp22icd	Same	Only FOM for TFC	No DN, DG. No residuals as desired
inp22ac8	Same	Only FOM for TFC	No DN, DG. Residuals tallied for ^{4}He, ^{7}Li, ^{9}Be, ^{10}Be are identical for d & dp.
inp22ic8	Same	Only FOM for TFC	No DN, DG. Residuals tallied for ^{4}He, ^{7}Li, ^{9}Be, ^{10}Be are identical for d & dp.

5.4.6. ACIC subset 4f.

Test problems 4f contains ^{6}Li, a 10-MeV neutron source, and the phys and act cards

```
phys:n 3j -1 2j 2   $ Analog sampling, libs only, Li+NCIA.
phys:p 5j -102      $ MG + Line.
act nonfiss=p
```

This model tests the residual tally for the ^{6}Li(n,α)^{1}H+2n and ^{6}Li(n,^{1}H)^{6}He reactions. There is no DN or DG production for this model. As indicated in Table 4f, the results look good. Some differences between MCNP6p and v270p are observed in the outp and mctal files for the "if the largest history score sampled so far were to occur on the next

history, the tfc bin quantities would change as follows" figure-of-merit values. The residual tallies are identical for MCNP6p and v270p, for the respective AC and IC calculations, as desired. The residual tallies for the AC and IC are in reasonable agreement.

Table 4f. Results for analog and implicit capture inp23 series test models.

Test Model	Results for MCNP6p and v270p		
	Problem Summary table	mctal file	Other
inp23ac	Same	Only FOM for TFC	Same ^{1}H, ^{4}He, ^{6}He residual tally for d & dp
inp23ic	Same	Only FOM for TFC	Same ^{1}H, ^{4}He, ^{6}He residual tally for d & dp.

5.5. Test Set 5: Beddingfield photofission HEU verification models.

Details of the models that have been developed as validation tests involving neutron sources have been previously reported (Durkee et al., 2009b). No experimental results were reported for photofission. Here we use the neutron-fission models for verification tests. The HEU and Pu targets are irradiated with 12-MeV photons.

The calculations are executed for DN production by ACE data (dnb=–1) or C90 model (dnb=–101), DG production by data (CID nflag=1) or model (CEM nflag=2), and DG production by line (dgb=-102), MG (dgb=–101), or off (dgb=0). The DG production by data ("Data") calculations (nflag=1) use the data card entry "pnlib=70u", whereas for production by model ("Model", nflag=2) "pnlib=99u" is used so that CEM is invoked.

Print triggers show that the majority of entries to CID cause model photofission (nflag=2, CEM providing the residuals). However, in some instances table fission (nflag=1) occurs for neutrons.

Selected results are given in Table 5.

Table 5. Delayed photon and neutron creation because of particle decay for HEU photofission by 12-MeV photons (from outp problem summary table). nps=1000 for Line, 200000 for multigroup (MG), 200000 for DN only (DN). DN production via ACE (dnb =–1) or CINDER'90 (dnb=–101). DG integration schemes Line (dgb=–102), multigroup (dgb=–101), no DG (dgb=0). DG production schemes Data (nflag=1) and Model (nflag=2).

DN Production Scheme	DG Production Scheme	DG Integration Scheme	DG Tracks		DN Tracks	
			MCNP6p	v270p	MCNP6p	v270p
ACE	Data (nflag=1)	1.Line	2284	2270	1	0
		2.MG	662216	664291	32	32
		3.DN	0	0	22	25
	Model (nflag=2)	4.Line	610	595	0	0
		5.MG	132999	132606	16	20
		6.DN	0	0	10	13
C90	Data (nflag=1)	7.Line	2288	2262	14	15
		8.MG	665586	664762	2094	2080
		9.DN	0	0	1650	1656
	Model (nflag=2)	10.Line	579	571	5	5
		11.MG	132651	132668	470	477
		12.DN	0	0	463	470

The MCNP6p and v270p results are in close agreement. However, the following observations are made. These observation are drawn in concert with the results given in Table 6 for neutron fission.

- DN creation in ACE will not include photofission-induced production (Lines 1-6). Thus, these DN production values are artificially low.

- In contrast, DN production in CID will give photofission-induced production (Lines 7-9). DN production via CEM creation of the residuals and CID for DN creation (Lines 10-12) is better than ACE-based DN (Lines 4-6), but is subdued versus Data-based sampling of the fission residuals (Lines 7-9) because CEM oversamples activation and undersamples fission-residuals.[†]
- DN production is significantly greater for Line 8 than Line 9. This stems from gamma production for MG, which in turn causes additional photofission and the subsequent boost of DN production.

5.6. Test Set 6: Beddingfield neutron fission verification models.

MCNP6p and v270p have been executed with neutron fission of the HEU and Pu models (Beddingfield and Cecil, 1998; Durkee et al., 2009b). These models specify 0.025-eV neutrons incident on HEU and Pu targets. Calculations were completed to examine DNDG production, with the DN production done using ACE data (dnb=–1) and C90 model (dnb=–101) techniques.

- The results obtained using MCNP6p and v270p are very similar.

- DG creation DG production by model (nflag=2, rows 4,5 and 10,11) is approximately 10% less than production using data (nflag=1, rows 1, 2 and 7, 8 of Table 6). This occurs because (print triggers show that) single residuals, ^{234}U,

[†] These observations supercede those drawn in Durkee, June 2011.

^{235}U, and ^{236}U are sent to CID by CEM. These residuals are all stable (half-lives greater than 100 times the maximum d-array value), so there are no DGs produced for these nuclides via the model leg. DG production is limited to the data leg (nflag=1), which has the same entries as calculations executed using data only.

- Using outp file weight-per-source-particle data, $\bar{\beta}$ is 6.6550e-3/(6.6550e-3+8.6678e-1) = 7.62e-3 and 6.9800e-3/(6.9800e-3+8.6667e-1) = 7.99e-3 for MCNP6p and v270p, respectively. These $\bar{\beta}$ values are reasonable—Lamarsh (1972, p.100) gives 0.0065 for thermal fission of ^{235}U and .0148 for fission of ^{238}U induced by a fission spectrum.

- DN production by fission (Table 6, Lines 2&3, 5&6) is much greater than photofission (Table 5, Lines 2&3, 5&6) because ACE does not treat photofission-induced DN production. Thus the relative results are as expected.

- DN production in Lines 8 exceeds that in Line 9 differ due to photofission-boosted DN production that is accounted for in CID using Data sampling of the photofission residuals.

- DN production in Lines 11&12 is less than Lines 8&9 because CEM oversamples activation and undersamples photofission residuals.

Table 6. Delayed photon and neutron creation because of particle decay for HEU neutron fission by 0.025-eV neutrons (from outp problem summary table). nps=1000 for Line, 200000 for multigroup (MG), 200000 for DN only (DN). DN production via ACE (dnb = –1) or CINDER'90 (dnb= –101). DG integration schemes Line (dgb = –102), multigroup (dgb = –101), no DG (dgb = 0). DG production schemes Data (nflag=1) and Model (nflag=2).

DN	DG Production Scheme	DG Integration Scheme	DG Tracks		DN Tracks	
			MCNP6p	v270p	MCNP6p	v270p
ACE	Data (nflag=1)	1.Line	2583	2564	3	3
		2.MG	844318	843830	1256	1257
		3.DN	0	0	1244	1244
	Model (nflag=2)	4.Line	2205	2205	3	3
		5.MG	656941	656885	1191	1191
		6.DN	0	0	1183	1183
C90	Data (nflag=1)	7.Line	2675	2680	10	9
		8.MG	842893	842348	2076	2078
		9.DN	0	0	1544	1543
	Model (nflag=2)	10.Line	2336	2336	8	8
		11.MG	655541	655447	1397	1396
		12.DN	0	0	1388	1391

5.7. Test Set 7: ^{17}O 15-MeV neutron activation verification models.

Six additional models are used to examine DNDG production arising from 15-MeV neutrons interacting with ^{17}O. Execution using MCNP6p and v270p gives essentially the same DG production for all schemes. Execution using ACE data gives zero DN production, as desired, because ACE treats only fission—DN production for activation is not treated using the ACE DN option. This model creates single (nzero=1) residuals (one per activation event) and tests the top activation product dynamic list treatment for DG emitters and the non-DG-emitter ^{14}C. Despite not emitting DGs, ^{14}C is retained as a top AP so that it does not require repeated CDF calculation (via sampf1 & C90) for DG

emission. Repeated CDF calculation would dramatically slow execution. Other SMR models (see, e.g., the preceding Section 6.2) have residuals that are all DG emitters; thus, this ^{17}O serves a useful validation purpose. Selected DNDG calculated results for MCNP6 and v270p are listed in Table 7.

Table 7. Delayed photon and neutron creation because of particle decay for ^{17}O neutron irradiation by 15-MeV neutrons (from outp problem summary table). nps=1000 for Line, 200000 for multigroup (MG), 200000 for DN only (DN). DN production via ACE (dnb = –1) or CINDER'90 (dnb= –101). DG integration schemes Line (dgb = –102), multigroup (dgb = –101), no DG (dgb = 0). DG production scheme Model (nflag=2).

DN	DG Production Scheme	DG Integration Scheme	DG Tracks		DN Tracks	
			MCNP6p	v270p	MCNP6p	v270p
ACE	Model (nflag=2)	1.Line	3670	3670	0	0
		2.MG	3580	3580	0	0
		3.DN	0	0	0	0
C90	Model (nflag=2)	4.Line	3662	3662	6297	6297
		5.MG	3572	3572	6297	6297
		6.DN	0	0	6297	6297

5.8. Beddingfield neutron fission validation models.

To illustrate the MCNP delayed-particle feature, we present results here for models based on experiments that were conducted by Beddingfield and Cecil (1998). In their experiments, HEU and Pu targets were irradiated by a moderated ^{252}Cf neutron source. Following irradiation, the targets were moved to an HPGe detector for high-resolution measurements of delayed-gamma spectra.

We have previously reported (Durkee et al., 2009b) simulation results based on their experiments. Because many of the details of their experiments were not provided, we approximated their experimental arrangement using representative configuration parameters. Despite our modeling approximations, our simulation results yielded calculated spectra that agreed well with their measured data.

We use the same *in silico* setup for the present study. The Beddingfield and Cecil (1998) experimental setup was approximated using an MCNP model consisting of an HEU or plutonium disk (same specifications as the experimental samples). In the simulations, each disk was exposed to a 0.025-eV neutron pulse emitted inwardly from a spherical surface located at a radius 2.7 cm from the problem origin.

Because the experimental detector design details are not available (Beddingfield and Cecil, 1998), the physical detector was modeled using the specifications given in Knoll (2000). Figure 1 illustrates the MCNP simulation geometry.

Calculation One: Target irradiation and
delayed-particle surface-source-file creation.

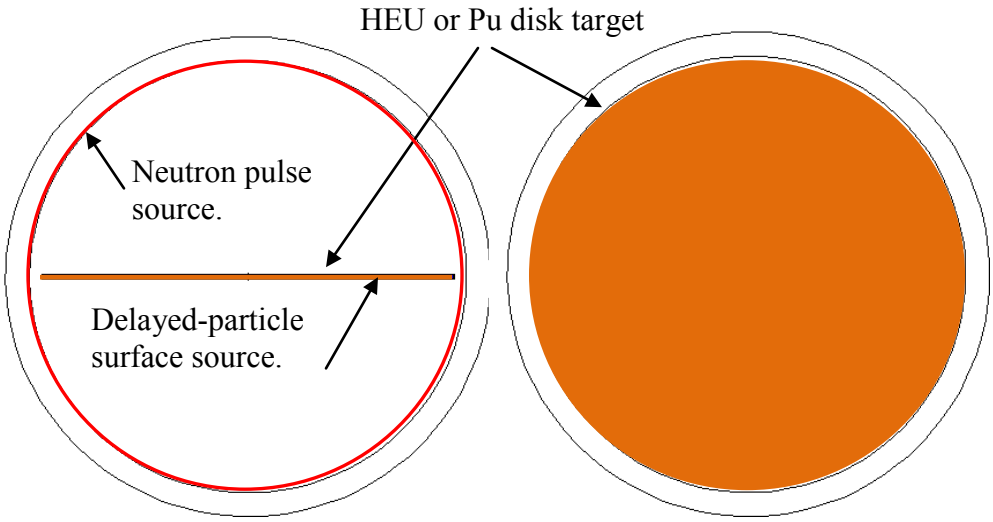

Calculation Two: Transport of delayed-particle surface source.

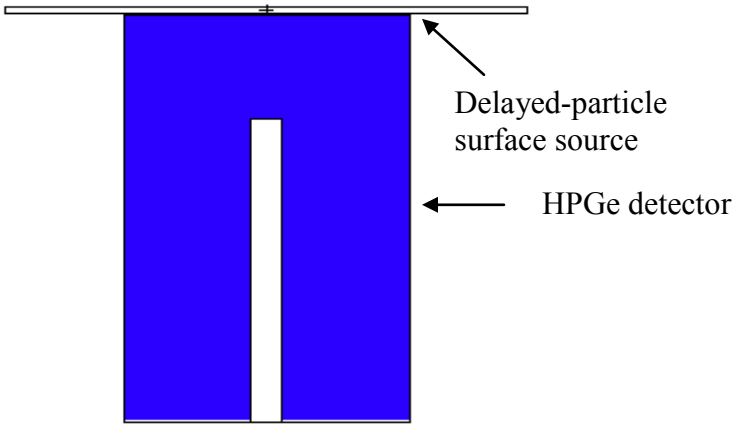

Figure 1. MCNP6 model approximating the Beddingfield and Cecil (1998) experimental setup. In each part-one calculation, a 0.025-eV neutron pulse is emitted inwardly from a 2.7-cm-radius spherical surface to induce fission in the HEU or Pu disk. Delayed particles emitted in the Early, Middle, or Late measurement time window after irradiation reaching the lower surface of the target are recorded in a surface-source file. In each part-two calculation, the surface source is read by MCNP6 and the delayed particles are transported to interact with the HPGe detector. Detector specs (radius = 1.4 cm, height = 4.50 cm) from Knoll (2000).

Simulations have been executed for each target to obtain delayed-gamma data. The simulations for each target and measurement period were done using two calculations that were designed to mimic the experimental procedure.

The first calculation performed irradiation of the target. Delayed particles emitted during the measurement period were "recorded" using the MCNP surface-source feature.[†] This feature writes information (including emission time, energy, direction, location) about the delayed gammas to a file (a "surface source" file). In these calculations, the surface source is located at the lower surface of the HEU or Pu disk target.

Following each irradiation calculation, the delayed-gamma surface source was "moved" to an *in silico* HPGe detector to measure the delayed-gamma activity. This second (measurement) calculation transported the photons from the surface-source to the detector. The MCNPX "F8" pulse-height tally was used to simulate the detector response.[*]

The F8 tally uses of the Gaussian energy broadening ("GEB") special feature ("FT"). The GEB feature is used to simulate the peak-broadening effects exhibited by physical radiation detectors using the expression FWHM = $a + b\sqrt{E + cE^2}$, where E is the particle

[†] The surface-source feature is standard with the general code release. The special modification writes the data to the surface-source file only for the stipulated time interval.

[*] The F8 (pulse-height) tally provides the energy distribution of pulses created in a cell that models a physical detector. The F8 energy bins correspond to the total energy deposited in a detector in the specified channels by each physical particle (history).

energy. For this study, the parameters (a, b, c) were (5.797×10^{-4} MeV, 7.192×10^{-4} $MeV^{1/2}$, 1.0 MeV^{-1}) ‡ (Princeton Gamma Tech, 2006).

All irradiation calculations were executed using the MCNP physics-model DNDG production techniques with the high-fidelity DG CDF integration scheme to provide high-resolution results. The calculations were executed using 200 million source histories.† These numbers of histories enables the 10 statistical tests to be passed for the total F8 tally, gives reasonable statistics for the F8 pulse-height tallies for the second (measurement) calculations, and results in relative uncertainties of < 0.20 for most of the prominent peaks.* The pulse-height tally calculations were obtained using 1-keV resolution (10^4 equal tally bins between 0 and 10 MeV). The pulse-height tally calculations were executed on a PC using a serial build and required only a few seconds of CPU time.

The validation calculations reported here were executed using MCNP6p and MCNPX v270p. This facilitates intercomparison of the results produced by each code, as well as comparison to the measured data. The first-stage irradiation/surface-source-creation

‡ The simulation used estimated values which should be representative of the Beddingfield and Cecil (1998) detector. The estimates were made using FWHM resolution at 0.122 and 1.33 MeV of 1 and 2 keV, respectively, presuming c=1.

† In addition, neutron transport was done using analog capture, rather than the default implicit capture for neutron transport, because the F8 pulse-height tally requires analog pulses. Execution also was done with fission and activation. Published results for MCNPX (Durkee, et al., 2009b) were executed using 200 MH, which causes reasonable agreement with the measured lower-amplitude peak data. Four 50-MH calculations were executed for the HEU and Pu models. The surface sources were transported to create mctal files. The mctal files were aggregated using the undocumented MCNPX arithmetic-tally feature, which is not yet available in MCNP6.

* The10 statistical checks provided by MCNPX for the aggregate (all energy bins) F8 tally are passed. The relative uncertainties for all prominent peaks are < 0.10 and < 0.20 for the low-lying peaks.

calculations were executed using Portland group MPI builds on the Pete cluster with 48-processor execution, and required roughly 10–15 hours per calculation. The second-stage surface-source transport/F8-tally calculations were executed on the PC, and required less than one minute per calculation.

5.8.1. Uranium model.

The Beddingfield and Cecil (1998) uranium experiment consisted of a thin disk (5.08-cm diameter, 0.05588-cm thickness) of material consisting of 93.15 at. % ^{235}U, 6.85 at. % ^{238}U and 100-s irradiation with a moderated ^{252}Cf source. Following irradiation, the sample was moved to an HPGe detector for delayed-gamma measurement 1050–1400 s following fission.

Figure 2a shows the HEU DG spectra that were measured (Beddingfield and Cecil 1998, Fig. 2) and calculated using MCNP6p. Figure 2b contains the HEU DG spectra that were measured (Beddingfield and Cecil 1998, Fig. 2) and calculated using MCNPX v270p. The MCNP6p and MCNPX v270p DG spectra results agree well with the measured data.

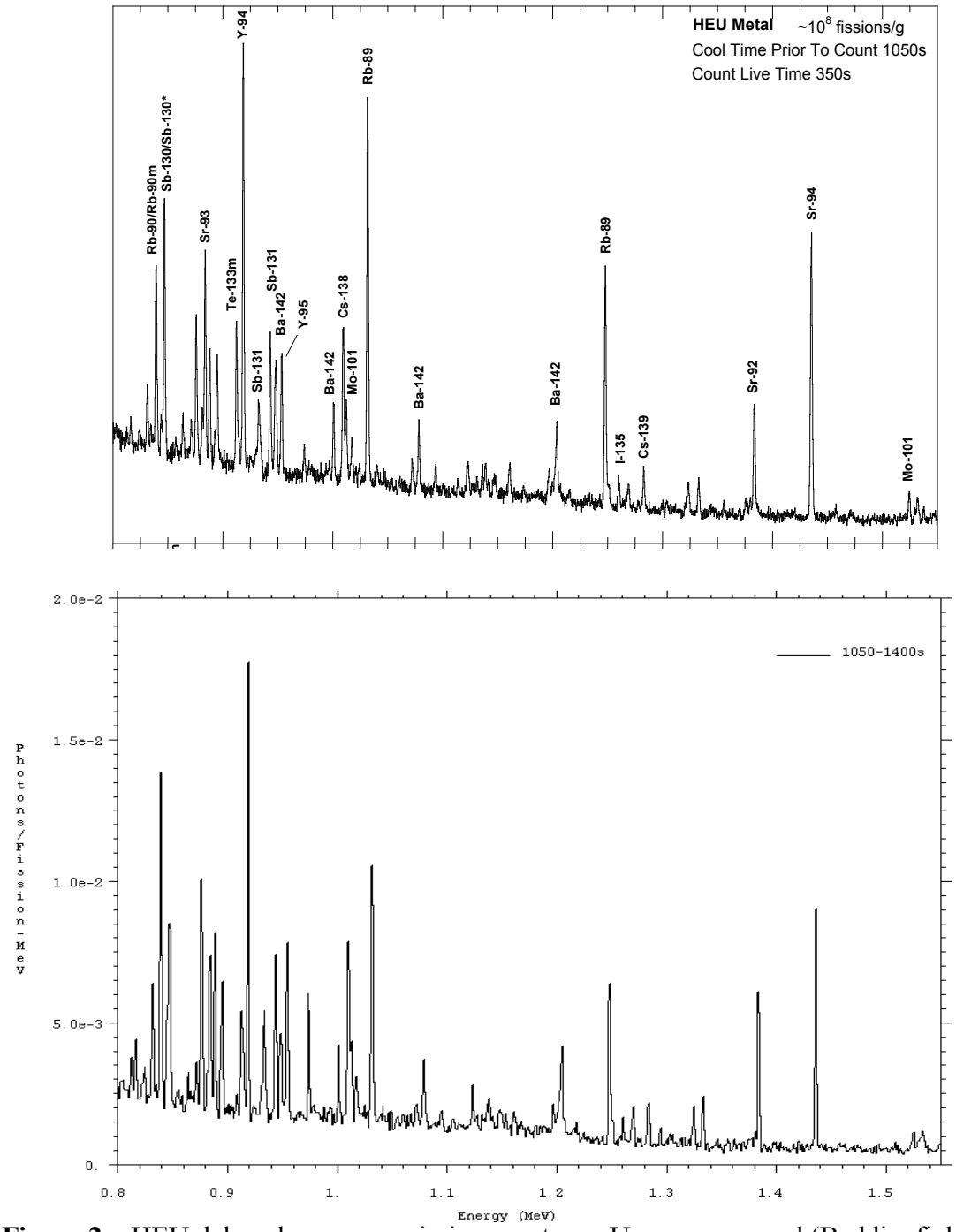

Figure 2a. HEU delayed-gamma emission spectrum. Upper: measured (Beddingfield and Cecil 1998, Fig. 2). Lower: calculated MCNP6p emission spectrum F8 pulse-height tally.

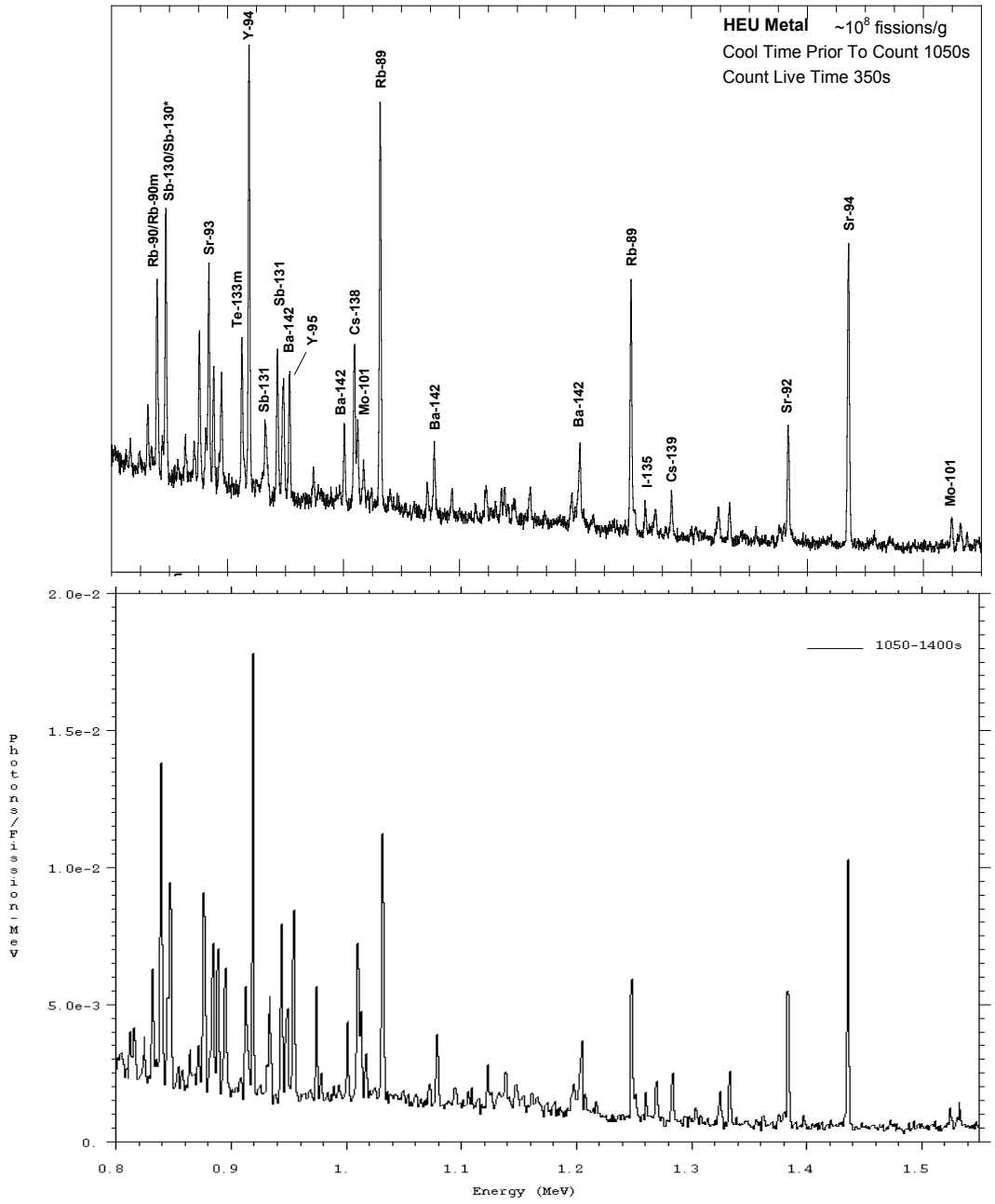

Figure 2b. HEU delayed-gamma emission spectrum. Upper: measured (Beddingfield and Cecil 1998, Fig. 2). Lower: calculated MCNPX v270p emission spectrum F8 pulse-height tally.

5.8.2. Plutonium model.

The Beddingfield and Cecil (1998) plutonium experiment closely resembles the uranium experiment. The plutonium disk (5.08-cm diameter, 0.05588-cm thickness) consisted of 98.97 at. % ^{239}Pu, 0.58 at. % ^{240}Pu, 0.0335 at. % ^{241}Pu, 0.0179 at. % ^{242}Pu, and was clad with 0.0508 cm of copper. The sample was irradiated for 100s using a moderated ^{252}Cf source. Following irradiation, the sample was moved to an HPGe detector for delayed-gamma measurement 1100–1450 s following fission.

Figure 3a shows the Pu DG spectra that were measured (Beddingfield and Cecil 1998, Fig. 2) and calculated using MCNP6p. Figure 3b shows the Pu DG spectra that were measured (Beddingfield and Cecil 1998, Fig. 2) and calculated using MCNPX v270p. The MCNP6p and MCNPX v270p DG spectra results agree well with the measured data.

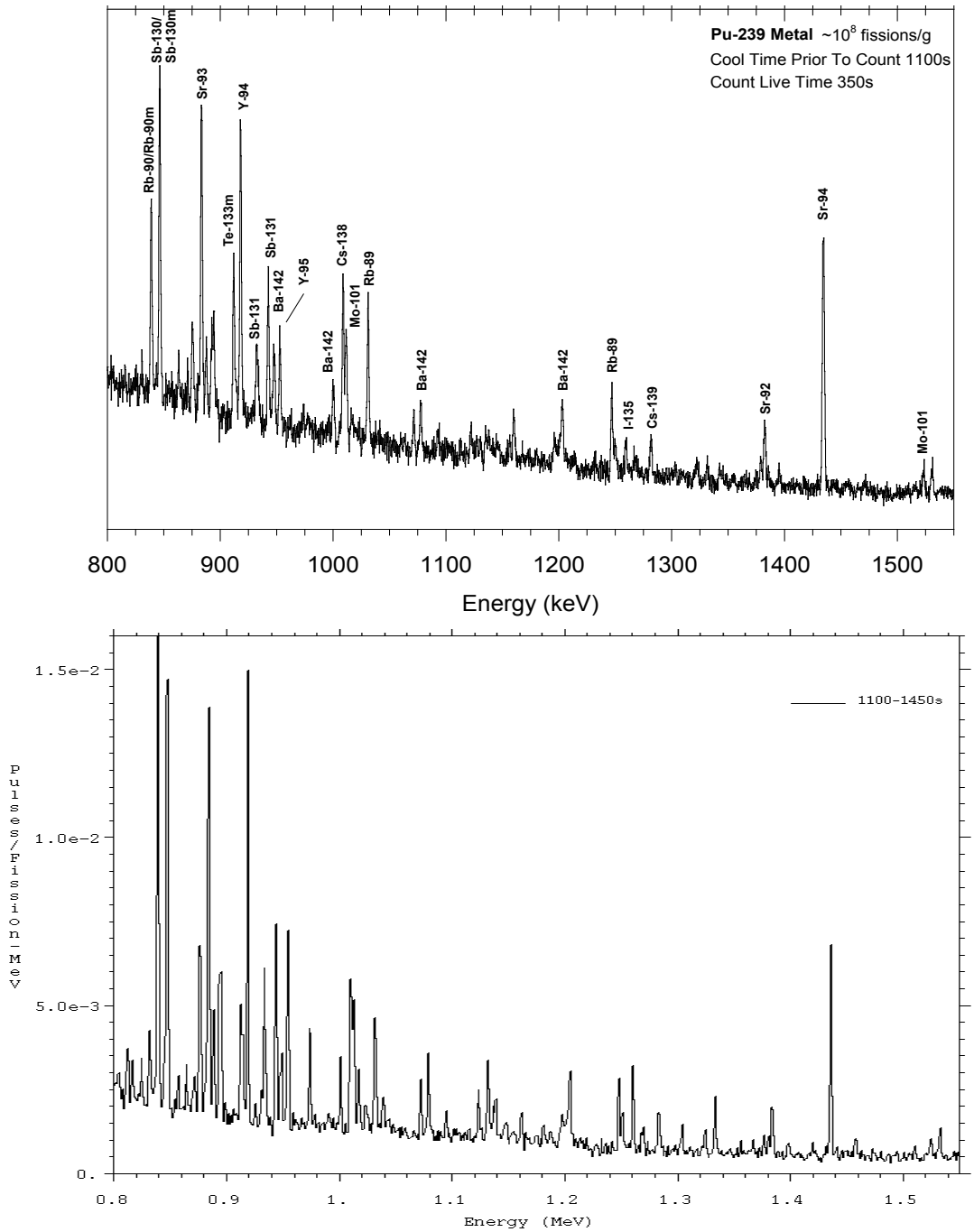

Figure 3a. Pu delayed-gamma emission spectrum. Upper: measured (Beddingfield and Cecil 1998, Fig. 2). Lower: calculated MCNP6p emission spectrum F8 pulse-height tally.

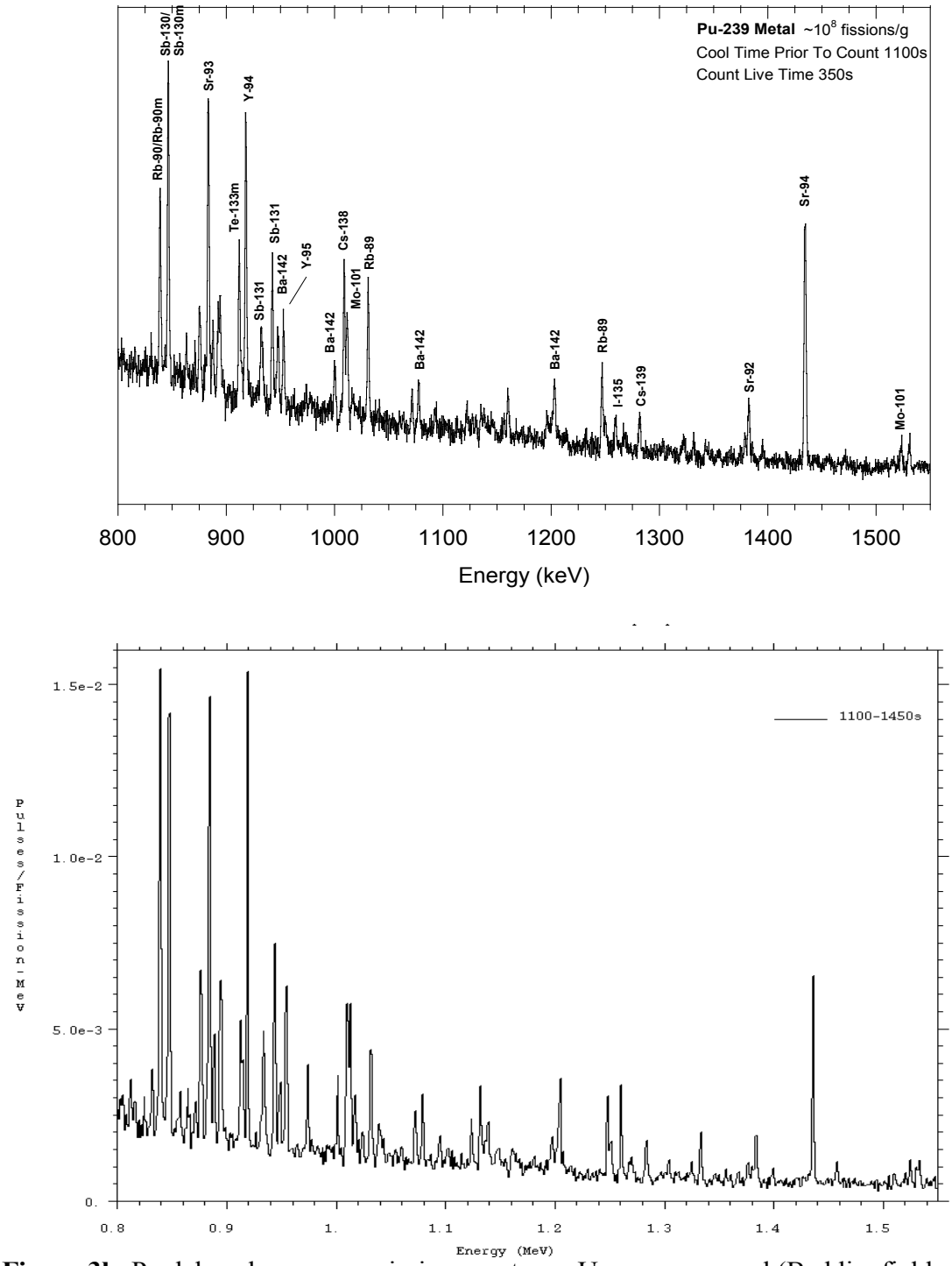

Figure 3b. Pu delayed-gamma emission spectrum. Upper: measured (Beddingfield and Cecil 1998, Fig. 2). Lower: calculated MCNPX v270p emission spectrum F8 pulse-height tally.

- Table 8 contains DG/fission data. Values for the weight per source particle give the same results as the track data in Table 8.

Table 8. Delayed gammas/fission for Beddingfield HEU & Pu neutron fission by 0.025-eV photons. DN production via CINDER90 model (dnb =–101). DG integration scheme Line (dgb=–102).

Beddingfield Model	outp photon creation by particle decay		outp neutron loss to fission		DG/fission	
	MCNP6p	v270p	MCNP6p	v270p	MCNP6p	v270p
HEU	118503086	118503080	17834127	17834126	6.65	6.65
Pu	93622536	93622534	15311973	15311972	6.11	6.11

6. Summary and conclusions

Almost six dozen test problems were executed to support the verification and validation effort for the MCNP6 delayed-particle (neutron and gamma) feature. As part of this effort, MCNP6 was patched with the latest fixes and modifications to address two principal issues. Issue 1 concerned differences between MCNP6 and MCNPX v270 coding (inaccurate transcriptions, missing code, etc.). Issue 2 pertains to upgrades developed for MCNPX in March, 2011, including 1) modification of the CINDER'90 CINDER interface routine (CID) to treat more than one residual for DNDG production by model (e.g., CEM and activation) and 2) DN production when DG production in not done for a particular fission or activation event.

Patched versions of MCNP6 (load date June 9, 2011 version 6.2.08) and MCNPX v270, here referred to as MCNP6p and v270p, were prepared with modifications to fix Issues 1 and 2. Execution of the test problems was done using using both patched codes to facilitate intercomparison of calculated results.

The test models used here have been created during the development of the delayed-neutron/delayed-gamma features beginning in 2005. The verification test models include fission, activation, analog and implicit capture, and residual tallies as well as delayed-gamma production by data and model. Recently (Durkee, June 2011), thirty new verification models were developed to focus testing for the fixes and modifications associated with Issue 2. Two validation models relate to the high-resolution delayed-gamma experiments for neutron-induced fission reported by Beddingfield and Cecil (1998).

Results for the verification models obtained using MCNP6p and v270p were in good agreement in all but one case. The inp01 test series, which tests delayed-particle and/or residual creation with neutron transport done using either analog and implicit capture, gives poor results. Debugging and code inspection indicates that the values for jptal and lft (basic tally info and pointers to the FT-card data, respectively) in subroutine talres.F90 are incorrect for MCNP6, differing from MCNPX. Mike James says this issue has not been fixed for MCNP6.

Execution of model o18lsw revealed that TOTNU was required. The requirement that TOTNU be used in (inp files for) models that treat activation without fission is not

intuitive. This pertains to execution using the June 9, 2011 code version. This issue has been resolved in the beta 2 code version—see below.

Results for the verification model ("DBP"), which has a reactivity of ~0.9, look good. The calculated $\bar{\beta}$ using Problem Summary table data is in reasonable agreement with data reported in the literature (Gozani, 2009; Lamarsh, 1972, p. 102; Sterbentz et al., 2007).

Beddingfield HEU and Pu validation models (Durkee et al., 2009b) were executed using a sufficient number of histories (200 million) to give F8 tallies with relative errors < 0.2 for most of the prominent peaks and for the total tally to pass the 10 statistical convergence tests. The MCNP6p and v270p results are in close agreement, and these results compare well with the experimental delayed-gamma spectra.

Because of the complexity and intricacies of the DNDG feature, numerous switches are used in MCNPX to guide execution. These switches enable delayed-particle production by data or model, CDF integration and storage schemes, treatment of residuals that are stable or lack high-fidelity DG line-emission data, single or multiple fission products or residuals, particle types (delayed neutrons and photons), analog or biased DN production, neutron transport analog or imlicit capture, and residual tallies. It is important that test calculations be executed using large numbers of histories to ensure functionality. Some of the verification calculations presented here have been executed for up to 10 million histories, and the validation calculations for 200 million histories.

The calculations and material discussed in this document were executed and prepared during the summer of 2011. **The MCNP6 beta 2 release in late 2011 changes the default TOTNU to "on". Thus, activation models that do not include fission no longer require the TOTNU card in order to produce delayed particles. The MCNP6 beta 2 release does not contain fixes for the residual tallies associated with delayed particles.** Additional validation calculations executed using the Beddingfield models are contained in, "The MCNP6 Delayed-Particle Feature" (LA-UR-12-00283) as a contribution for publication in J. of Nuclear Technology.

References

Beddingfield D.H. and Cecil F.E., 1998. "Identification of Fissile Materials From Fission Product Gamma-Ray Spectra**,**" Nuclear Instruments and Methods in Physics Research A; v. 417, pp. 405–412.

Bell G.I. and Glasstone S., 1970. *Nuclear Reactor Theory*, Van Nostrand Reinhold Company, Inc., New York, pp. 470–472.

Brown F.B., ed., April 2003a. "MCNP–A General Monte Carlo N–Particle Transport Code, Version 5, Volume I: Overview and Theory," Los Alamos National Laboratory report LA-CP-03-0245, Ch 2 pp. 182–185.

Brown F.B., ed., April 2003b. "MCNP–A General Monte Carlo N–Particle Transport Code, Version 5, Volume II: User's Guide," Los Alamos National Laboratory report LA-CP-03-0245, Ch 3 pp. 31–32.

Durkee Joe W., Jr., James M.R., McKinney G.W., Trellue H.R., Waters L.S., and Wilson W.B., 2009a. "Delayed-Gamma Signature Calculation for Neutron-Induced Fission and Activation Using MCNPX, Part I: Theory," Progress in Nuclear Energy, **51**, 813–827.

Durkee Joe W., Jr., McKinney Gregg W., Trellue Holly R., Waters Laurie S., and Wilson W.B., 2009b. "Delayed-Gamma Simulation Using MCNPX. Part II: Simulations," Progress in Nuclear Energy, **51**, 828-836.

Durkee J.W., Jr., McKinney G.W., Trellue H.R., Waters L.S., and Wilson W.B., 2009c. "Delayed-Gamma Simulation Using MCNPX," J. Nuclear Technology, **168**, 761–764.

Durkee Joe W., Jr., James M.R., McKinney G.W., and Waters L.S., 2010. "MCNPX Delayed-Gamma Feature Enhancements," Transactions of the American Nuclear Society, **103**, 651–652.

Durkee Joe W., Jr., February 2011. "MCNP6 Delayed-Particle Verification and Validation," Los Alamos National Laboratory report LA-UR-11-01375.

Durkee Joe W., Jr., June 2011. "MCNPX Delayed-Particle Verification and Validation," Los Alamos National Laboratory report LA-UR-11-03315.

Gozani T., 2009. "Fission Signatures for Nuclear Material," IEEE Transactions on Nuclear Science, **56**(3), 736–741.

Henry A.F., 1975. *Nuclear-Reactor Analysis*, MIT Press, Cambridge, Massachusetts, p. 324.

Hetrick D.L., 1971. *Dynamics of Nuclear Reactors*, University of Chicago Press, Chicago, pp. 441–448.

Lamarsh J.R., 1972. *Introduction to Nuclear Reactor Theory*, Addison-Wesley Publishing Co., Inc., Reading, Massachusetts, p. 93.

Massimo L., 1976. *Physics of High-Temperature Reactors*, Pergamon Press, New York, pp. 162–165.

Pelowitz D.B., ed., April 2011. "MCNPX User's Manual Version 2.7.0," Los Alamos National Laboratory report LA-CP-11-00438.

Sterbentz J.W., Jones J.L., Yoon W.Y., Norman D.R., and Haskel K.J., 2007. "Benchmark Validation Comparisons of Measured and Calculated Delayed Neutron Detector Responses for a Pulsed Photonuclear Assessment Technique," J. Nuclear Instruments and Methods in Physics Research B, **261**, 373–377.